Journal of the Serbian Chemical Society
JSCS-info@shd.org.rs • www.shd.org.rs/JSCS
J. Serb. Chem. Soc. 80 (12) 1529–1540 (2015)
JSCS–4817
UDC 546.462+661.183.8:66.091.7:
544.022:519.23:544.773.42/.43:536.5
Original scientific paper

Study of the effect of Mg(II) addition and the annealing conditions on the structure of mesoporous aluminum oxide using Plackett–Burman design

TATJANA B. NOVAKOVIĆ[1*#], LJILJANA S. ROŽIĆ[1#], SRĐAN P. PETROVIĆ[1#], ZORICA M. VUKOVIĆ[1] and MIODRAG N. MITRIĆ[2]

[1]ICTM-Department of Catalysis and Chemical Engineering, University of Belgrade, Njegoševa 12, Belgrade, Serbia and [2]Institute of Nuclear Sciences „Vinča“, University of Belgrade, Mike Petrovića Alasa 12–14, Belgrade, Serbia

(Received 13 November 2014, revised 26 June, accepted 6 July 2015)

Abstract: A statistical design was used to investigate the effect of various processing conditions on the structure of sol–gel derived Mg(II) doped alumina. Six process variables were selected based on the Plackett–Burman design: concentration of magnesium nitrate, time and temperature of alcohol evaporation, temperature and time of annealing and heating rate were changed at two levels. For every set of conditions, samples with different specific surface area and degree of crystallinity were obtained. Analysis of the results showed that the annealing temperature, heating rate and concentration of magnesium nitrate were the main factors affecting the average crystallite size of the predominant alumina phase. In the case of the specific surface area, two of selected six variables had pronounced effects; however, the temperature of annealing was more effective than others. The present results showed that the proposed model that uses crystallite size as a response variable is preferable to other research.

Keywords: magnesium-doped alumina; statistical design; sol–gel.

INTRODUCTION

Mesoporous alumina is a very interesting material with broad applicability as an adsorbent, coating, porous ceramics, catalyst, and catalyst support.[1–7] Active alumina does not occur naturally and it is primarily prepared by hydrothermal or thermal transformations of aluminum hydroxides or alumogel. During annealing, organic groups are removed and the gel transforms to a more stable solid phase. This evolution involves chemical modification, crystallographic trans-

* Corresponding author. E-mail: tnovak@nanosys.ihtm.bg.ac.rs
# Serbian Chemical Society member.
doi: 10.2298/JSC141113056N

formation of the solid matter, and reorganization of the solid network and of the pore geometry.[8]

At temperatures below 1000 °C, alumina phases that are often formed are not thermodynamically stable. The temperature of the transformation of metastable phases of alumina into α-Al_2O_3, which is the only thermodynamically stable phase, is influenced by various factors, such as particle size, morphology, crystalline form and organic and inorganic additives.[9] Additives have a great influence on the kinetics of the transformation. The addition of lanthanum species greatly improves the thermal stability, which inhibits the sintering and phase transformations of alumina.[3,10,11] Magnesia, which has a high melting point above 2500 °C, also affects the surface stability of alumina even at temperatures exceeding 1000 °C[7] and produces different accelerating effect depending on the initial surface area.[12] A few studies showed that alumina undergoes phase transformation with increasing calcination temperature, and that the average pore diameter increases with a high temperature while the pore volume and surface area should decrease until the pore structure collapses.[8,13] The performance of alumina as a catalyst or catalyst support largely depends on its crystalline structure, and chemical, and textural properties.[14–16] These properties of transformed alumina, such as morphology, and structural and textural characteristic, are affected not only by the synthesis methodology but also by the subsequent calcinations conditions.[17–21]

Although a large number of parameters could be modified during the preparation of alumina, a great majority of experimental studies on the synthesis of alumina use the conventional method.[22] The conventional multifactor experimental design requires only one variable to be changed at a time to determine its effect. However, when there are many parameters, this procedure may be very long and does not allow a clear identification and influence of linked parameters. These limitations of conventional method can be eliminated by optimizing the affecting parameters collectively by statistical experimental design. The Plackett–Burman (PB) design provides an efficient way for handling a large number of variables and identifying the most important ones. Therefore, this type of design is useful in preliminary studies.[23–25] The design analyzes the input data and presents a rank ordering of the variables with magnitude of effect and designates signs to the effects to indicate whether an increase in factor value is advantageous or not.[26] However, the simultaneous effect of parameters of sol–gel synthesis and calcinations conditions on the pore structure formation of Mg(II)-doped alumina has not been investigated. There are six parameters in the sol–gel synthesis and three calcination variables and thus, a great number of experiments should be simultaneously run, and their possible interactions should be studied.

The aim of this study was to examine the influence of a large number of variables on the structural properties of Mg(II)-doped alumina and to indentify

the most significant ones. PB experimental design at two levels was used to identify the key variables. A graphical display of data, Pareto charts and main effect plots can be used to find a relationship between the input variables and the system response.

EXPERIMENTAL

Preparation of Mg(II)-doped alumina

Mg(II) doped alumina was prepared by sol–gel method using aluminum alkoxide as a precursor. To prepare boehmite sols, aluminum isopropoxide was hydrolyzed in an excess amount of water (100:1, H_2O:Al^{3+} mole ratio) at 80 °C, followed by peptization with the appropriate amount of HNO_3 (0.07:1, H^+:Al^{3+} mole ratio) to form a stable colloidal sol.[27] The sol was kept at a constant temperature for the desired time under reflux conditions, during which most of the alcohol was evaporated. The freshly prepared boehmite sol and polyethylene glycol (PEG, mol. wt. 5600 g mol^{-1}, mol. radius 2.3 nm) or a variable concentration of magnesium nitrate solution combined with PEG, were mixed together and then vigorously stirred in order to obtain a homogeneous Mg(II)-doped boehmite sol. The doped boehmite sols were then gelled at 40 °C. The gels were heated from room temperature to the final temperature, which ranged between 500 and 1100 °C. The heating rate ranged between 2 and 10 °C min^{-1}. The samples were kept at final temperatures for a fixed period, which ranged from 1 to 10 h.

Experimental design

In this study, a PB design was applied for twelve trials in order to evaluate the significance of six variables on the formation of Mg(II)-doped alumina. The independent variables screened were annealing temperature (X_1), heating rate (X_2), time of annealing (X_3), concentration of magnesium nitrate (X_5), time of the evaporation of alcohol (X_7) and temperature of the evaporation of alcohol (X_9). Each independent variable was tested at two levels, a high and a low level, which were denoted by (+1) and (–1), respectively (Table I). Dummy variables (X_4, X_6 and X_8) were employed to evaluate the standard errors of the experiment.

TABLE I. Variables and levels used in the PB experimental design matrix

Variable	Symbol	Unit	Low (–1)	High (+1)
Annealing temperature	X_1	°C	500	1100
Heating rate	X_2	°C min^{-1}	2	10
Time of annealing	X_3	h	1	10
Concentration of Mg(II)	X_5	mol Mg/mol Al_2O_3	0.03	0.06
Time of evaporation	X_7	h	60	72
Temperature of evaporation	X_9	°C	85	95

The data obtained from the PB design experiments were analyzed using Minitab 16 statistical package software trial version (Pennsylvania State University).

The main effect of each variable was calculated as the difference between the average of measurements made at the high and low levels of that factor. The PB design is based on the first order model:

$$Y = b_0 + \sum b_i X_i \quad (1)$$

where Y is the predicted response, X_i are the input variables that affect the response Y, b_0 is the intercept term and b_i are the linear terms. This model does not describe interaction among factors and it is used to screen and evaluate the important factors that influence the response.[24]

Characterization of Mg(II)-doped alumina

The phase structure of the samples after the thermal treatments was studied by the X-ray diffraction method (Philips PW 1710 powder diffractometer with CuK_α radiation (40 kV, 30 mA, λ = 0.154178 nm)) in the 2θ range from 3 to 70°. The crystallite size was determined from XRD patterns using the Scherer equation:

$$D = \frac{0.9\lambda}{\beta \cos\theta} \tag{2}$$

where D represents the crystallite size in nm, λ is the CuK_α radiation wavelength, β is the full width at half maximum in radian and θ is the Bragg angle.

Nitrogen adsorption was performed at –196 °C in the relative pressure interval between 0.05 and 0.98 using an automatic adsorption apparatus (Sorptomatic 1990 Thermo Finningen). Before each measurement, the sample was degassed at 250 °C under vacuum for a sufficient time (4 h < t < 10 h) to observe the absence of significant changes in vacuum stability. The adsorbed amount of nitrogen was measured by volume at standard temperature and pressure. The specific surface areas S_{BET} *a*nd C were calculated by the BET method[28-30] from nitrogen adsorption–desorption isotherms, using data up to p/p_0 = 0.3, and the pore size distribution was computed from the desorption branch of the isotherms.[30]

RESULTS AND DISCUSSION

The Plackett–Burman (PB) design enabled the influence of the six variables to be established with only twelve experiments. This optimized method permits an estimation of the main effects of the variables and disregards interactions between them. The twelve experiments were summarized in the matrix and are listed in Table II.

TABLE II. PB experimental design matrix with the responses specific surface area (Y_1) and crystallite size (Y_2)

Run	X_1	X_2	X_3	X_4	X_5	X_6	X_7	X_8	X_9	Y_1	Y_2
1	1	–1	1	–1	–1	–1	1	1	1	10.0	90.7
2	1	1	–1	1	–1	–1	–1	1	1	79.9	58.4
3	–1	1	1	–1	1	–1	–1	–1	1	275.6	6.4
4	1	–1	1	1	–1	1	–1	–1	–1	35.8	84.1
5	1	1	–1	1	1	–1	1	–1	–1	84.5	48.8
6	1	1	1	–1	1	1	–1	1	–1	14.5	52.3
7	–1	1	1	1	–1	1	1	–1	1	279.1	14.7
8	–1	–1	1	1	1	–1	1	1	–1	301.6	8.5
9	–1	–1	–1	1	1	1	–1	1	1	285.3	12.2
10	1	–1	–1	–1	1	1	1	–1	1	76.4	68.2
11	–1	1	–1	–1	–1	1	1	1	–1	307.2	21.3
12	–1	–1	–1	–1	–1	–1	–1	–1	–1	315.7	19.5

From the nitrogen adsorption–desorption isotherms, the specific surface area (Y_1 / m^2 g^{-1}) for all Mg(II)-doped alumina samples were calculated. The obtained results are presented in Table II and used as a dependent variable (Y_1) in the PB design. The second response in the PB design was crystallite size (Y_2 / nm), determined from the XRD patterns using Eq. (2).

The specific surface areas obtained for each combination of the variables were calculated from the nitrogen adsorption–desorption isotherms shown in Fig. 1, whereby a wide variation in the specific surface area from 316 to 10 m^2 g^{-1} was found.

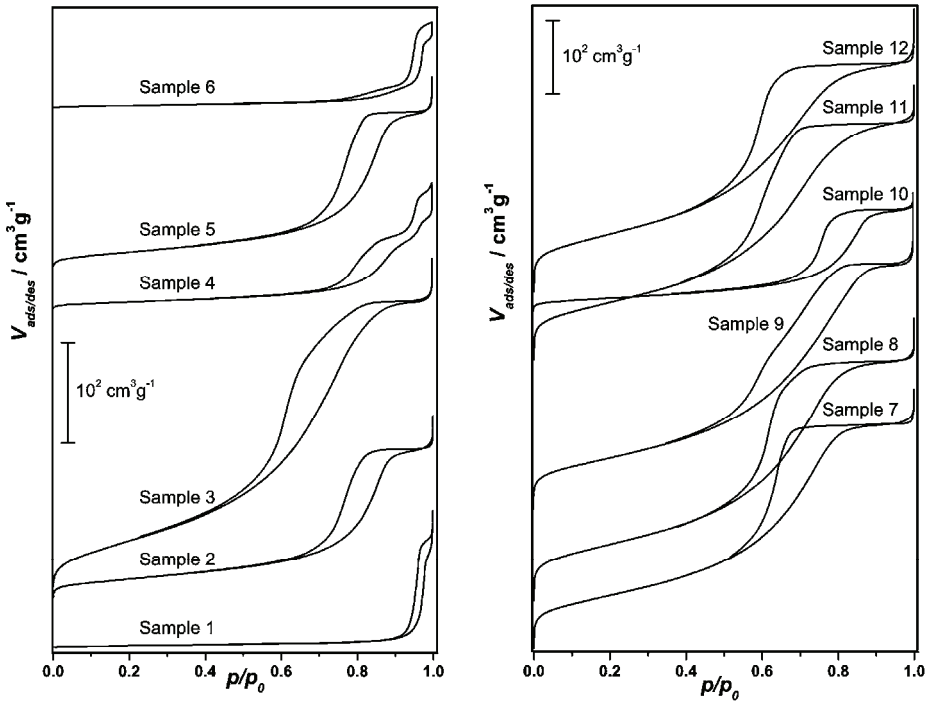

Fig. 1. Nitrogen adsorption–desorption isotherms for the Mg(II)-doped alumina samples.

The alumina samples obtained in experiment 3, 7–9, 11 and 12 annealed at 500 °C were characterized by a type IVa isotherm with a hysteresis loop of the H2 type, indicating the presence of mesopores, within a well-defined pore shape type.[28,30] The samples 1, 2, 5 and 10 annealed at 1100 °C could be described as having type IVa isotherm, the initial region of which was closely related to Type II isotherms, leveling off at high relative pressures with a characteristic saturation plateau, although this could be short and reduced to an inflexion point. A type IVa isotherm is encountered when adsorption occurs on low porosity material or on material with mostly mesoporous pore diameters. The isotherms for samples 4

and 6 were stepwise (Type VI), which are associated with layer-by-layer sorption on a highly uniform surface. The isotherms for samples 4 and 6 also showed hysteresis on the desorption isotherm curve with a smaller desorption step. Although samples 1, 2, 4–6 and 10 were all annealed at 1100 °C, sample 2, 5 and 10 aluminas show different specific surface area compared to samples 1, 4 and 6. These results highlight that the specific surface area of alumina samples depends not only on the annealing temperature, but also on the heating rate and the period in which they were kept at this temperature.

The plot of the pore size distribution (Fig. 2) shows two regions of pore size. The first one reflects a very narrow distribution of mesopores with diameters between 4.9 and 5.7 nm. The smaller average diameter and homogeneity of the mesopores were obtained in experiments 3, 7, 8, 9, 11 and 12 in comparison with the samples annealed at 1100 °C (experiment 1, 2, 4–6 and 10). With increasing annealing temperature, the maximum in pore size distribution was shifted to a larger pore diameter and the distribution became broader, as shown in Fig. 2. The samples obtained in experiments 1, 4 and 6 showed bimodal distributions, characteristics for the spinel structure of magnesium aluminates.[5] These distributions describe the charge transferring pores with radius 5 nm depending on annealing conditions and water exchange inside-delivering or communication mesopores with radius 10 nm, depending on the specific surface area of the Mg(II)-doped alumina. Thus, it could be concluded that the synthesis of bimodal porous alumina depended not only on the annealing temperature, but also on the concentration of magnesium nitrate, heating rate and period for which they were kept at this temperature.

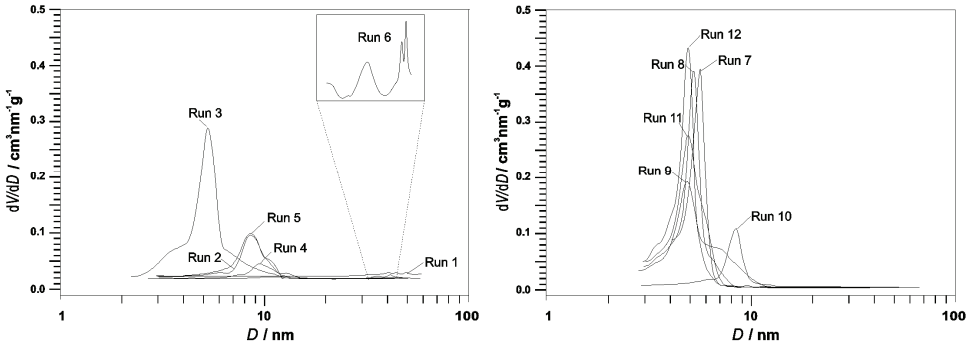

Fig. 2. Pore size distributions of Mg(II)-doped alumina samples.

The XRD patterns (Fig. 3) identified η-Al_2O_3 (PDF-2: 77-0396), γ-Al_2O_3 (PDF-2: 75-0921) and θ-alumina (PDF-2: 86-1410) as crystalline phases for the samples obtained in the experiments 3, 7–9, 11 and 12. X-Ray diffraction could not clearly distinguish between η- and γ-Al_2O_3 and thus, they will be denoted as γ-Al_2O_3. Besides θ-Al_2O_3 in the case of the samples obtained in the experiment

2, 5 and 10, δ-Al_2O_3 (PDF-2: 46-1215) was identified. Lines detected at 25.5, 34, 36.6 and 50.8° related to the presence of well crystalline α-Al_2O_3 (PDF-2: 74--1081) obtained in experiments 1, 4 and 6. In addition, the magnesium aluminate spinel phase ($Mg_{0.4}Al_{2.4}O_4$, PDF-2: 84-0378) was identified in the samples from these experiments. The X-ray diffraction pattern analysis indicated that the formation of $Mg_{0.4}Al_{2.4}O_4$ starts at a temperature of about 1100 °C. These results are in good agreement with those of Orosco *et al.*[31]. In addition, it was observed that the larger degree of crystallinity is detected in samples obtained in experiment 1, 4 and 6 compared to the other samples. The stronger diffraction peaks for these samples suggest that they underwent a higher degree of phase transformation.

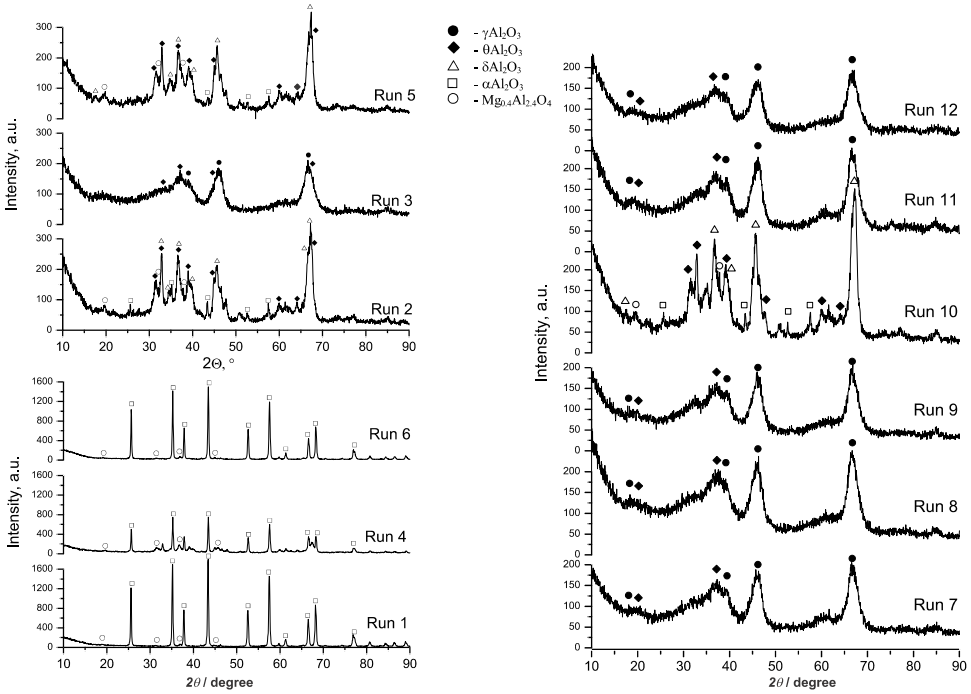

Fig. 3. XRD patterns of the Mg(II)-doped alumina samples.

The average crystallite size (Table II), which may be a good indicator of how surface area changed in Mg(II)-doped alumina under these experimental conditions, increased with increasing annealing temperature. There was a clear difference between the samples annealed at 500 °C (experiment 3, 7–9, 11 and 12) and those obtained at 1100 °C (experiment 1, 2, 4–6 and 10). However, the observed peaks for samples (experiment 3, 8 and 9) were very broad, which could be attributed to disordered arrangement of the very small crystallites making up the pores. Indeed, the calculated mean crystallite sizes according to the Scherer equation were approximately 6–12 nm. For all samples, the mean

crystallite size of the $\gamma(\eta)$-Al_2O_3 phase varied in the range 6.4–21.3 nm, while for the α-Al_2O_3 phase, it was up to 90 nm.

The phase transformations are accompanied by changes in the porous structure of Mg(II)-doped alumina. At higher temperatures (1100 °C), the formation of larger pores was notable, probably due to the collapse of the pores with shrinkage of the material structure. This also resulted in a strong increase in crystallite size and decrease in the surface area and pore volume.[8] The rapid collapse of the fine mesoporous structure started as conversion to the stable α-Al_2O_3 phase occurred at 1100 °C.

In order to determine the influence of the most important variables, a standardized Pareto chart (Fig. 4) was employed. It consists of bars with a length proportional to the absolute value of the estimated effects, divided by the standard error. The bars are displayed in order of the magnitude of the effects, with the largest effect at the top. Moreover, the chart includes a vertical line at the critical *t*-value, and the effect of its bar is smaller than the critical *t*-value is considered as not significant and not affecting the response variable.

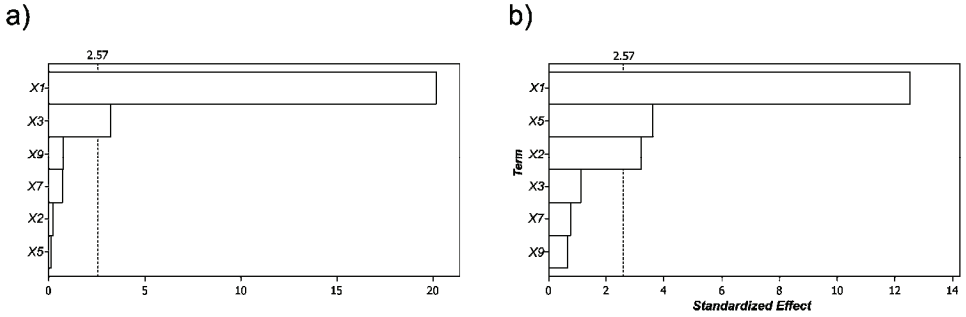

Fig. 4. Pareto chart of the estimated effects of six variables on: a) specific surface area (Y_1) and b) crystallite size (Y_2); $\alpha = 0.05$.

The Pareto chart (Fig. 4a) revealed that the annealing temperature (X_1) had the maximum standardized effect at 95 % confidence interval, while the heating rate (X_2), the concentration of magnesium nitrate (X_5), the time of alcohol evaporation (X_7) and temperature of alcohol evaporation (X_9) did not have a significant effect on the specific surface area. These findings were comparable with reports of Huang *et al.*[18] who investigated the influence of some operation parameters, *i.e.*, calcination temperature and time, and heating rate on the surface area, pore volume and pore size of alumina.

The Pareto chart for the variable Y_2 is presented in Fig. 4b, which confirmed that three variables were very significant: temperature of annealing (X_1), heating rate (X_2) and concentration of magnesium nitrate (X_5). The influences of the

other independent variables on this response were evaluated as having insignificant effects over the studied range of the variables.

In contrast to the Pareto chart, which compares absolute values of the effects, the main effect plot (Fig. 5) provides additional information on whether a change between the two variables levels decreases or increases the response.

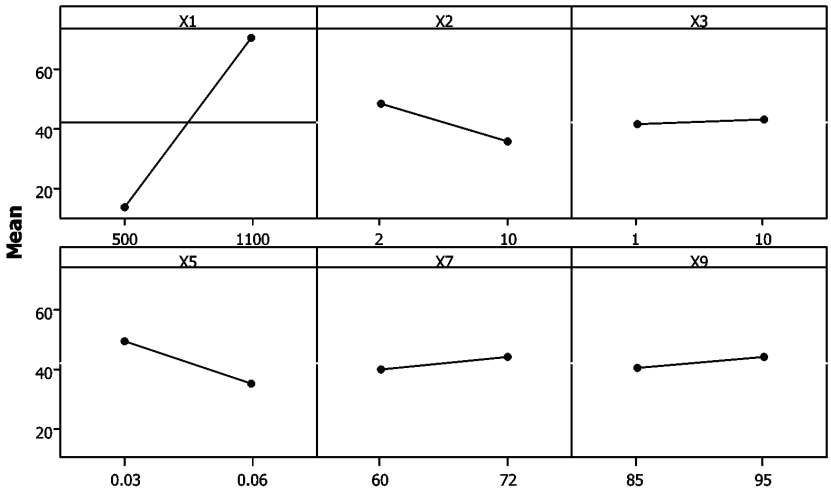

Fig. 5. Main effect plots for Y_2; data given are mean values.

The main effect plot illustrates the trends of all effects and it shows that increasing the annealing temperature leads to an increase in crystallite size, but decreases of the other variables results in the formation of small crystallites. Furthermore, the thermal shock caused by the high heating rate may accelerate the dehydration process, creating structure of magnesium aluminate spinel phase ($Mg_{0.4}Al_{2.4}O_4$) and leading toits formation.

The analysis of variance (ANOVA) was applied to test the suitability of PB design for the response Y_2 and the results are given in Table III.

TABLE III. Effects of the variables and statistical analysis of the PB design

Variable	Symbol	Effect	Coefficient	*P*-value
Annealing temperature	X_1	53.317	26.658	0.000
Heating rate	X_2	–13.550	–6.775	0.024
Time of annealing	X_3	4.717	2.358	0.318
Concentration of Mg(II)	X_5	–15.383	–7.692	0.015
Time of evaporation	X_7	3.217	1.608	0.484
Temperature of evaporation	X_9	2.683	1.342	0.556

P-values lower than 0.05 indicate that the model term is statistically significant. Analysis of the *P*-values showed that among the variables tested, the

temperature of annealing, heating rate and the concentration of magnesium nitrate had significant effects on the crystallite size. The model equation obtained from PB regression analysis for predicting the crystallite size could be written as:

$$Y_2 = -42.151 + 0.089X_1 - 1.694X_2 + 0.524X_3 - 512.778X_5 + \\ +0.268X_7 + 0.268X_9 \quad (3)$$

The model was found to fit adequately all experimental data with a coefficient of determination (R^2) of 0.9733, which indicates that 97.33 % of the variability of the response could be explained by the model. At the same time, the adjusted coefficient of determination R^2_{Adj} (0.9413) was also very high, which indicates the high significance of the model.

CONCLUSIONS

Mg(II)-doped alumina was prepared by the sol–gel method. The PB-design that was applied in this study could identify the main factors from a large number of variables in the synthesis of Mg(II)-doped alumina for the desired response variables. The results obtained from the present investigation revealed that the temperature of annealing, heating rate and concentration of magnesium nitrate were found to affect the crystallite size of the predominant phase of alumina. Among selected variables, annealing temperature was found to be the most significant parameter affecting the structural properties of alumina for both dependent variables. The fundamental information and this design were supportive for preliminary studies where the aim was to identify variables that could be fixed or modified in further investigations.

Acknowledgement. This work was supported by the Ministry of Education, Science and Technological Development of the Republic of Serbia (Project Nos. 172015 and 172001).

ИЗВОД

ПРОУЧАВАЊЕ УТИЦАЈА ДОДАТКА МАГНЕЗИЈУМА И УСЛОВА ТЕРМИЧКЕ ОБРАДЕ НА СТРУКТУРНА СВОЈСТВА МЕЗОПОРОЗНОГ АЛУМИНИЈУМ-ОКСИДА ПРИМЕНОМ PLACKETT–BURMAN ДИЗАЈНА

ТАТЈАНА Б. НОВАКОВИЋ[1], ЉИЉАНА С. РОЖИЋ[1], СРЂАН П. ПЕТРОВИЋ[1], ЗОРИЦА М. ВУКОВИЋ[1] и МИОДРАГ Н. МИТРИЋ[2]

[1]*ИХТМ-Центар за катализу и хемијско инжењерство, Универзитет у Београду,Његошева 12, Београд и* [2]*Институ за нуклеарне науке "Винча", Универзитет у Београду, Мике Петровића Аласа 12–14, Београд*

Применом статистичког дизајна проучаван је утицај услова синтезе сол–гел поступком и термичке обраде на структурна својства алуминијум оксида са додатком Mg(II). На основу Plackett–Burman дизајна извршен је избор процесних параметара који показују значајан утицај на структурна својства добијених узорака. Шест процесних варијабли: концентрација магнезијум-нитрата, време и температура испаравања алкохола, температура и време термичке обраде и брзина загревања су варирани на два нивоа. Као излазни параметри посматрани су: специфична површина синтетисаних узорака и величина кристалита доминантне фазе алуминијум-оксида. Резултати су показали да темпе-

ратура и брзина термичке обраде и концентрација магнезијум-нитрата имају најзначајнији утицај на средњу величину кристалита доминантне фазе алуминијум-оксида, док на вредности специфичне површине доминантан утицај има температура термичке обраде. Свеобухватна анализа добијених резултата показала је да је предложени модел који користи величину кристалита као излазни параметар погоднија за даља истраживања.

(Примљено 13. новембра 2014, ревидирано 26. јуна, прихваћено 6. јула 2015)

REFERENCES

1. E. J. A. Pope, J. D. Mackenzie, *J. Non-Cryst. Solids* **87** (1986) 185
2. S. M. Maliyekkal, A. K. Sharma, L. Philip, *Water Res.* **40** (2006) 3497
3. T. Novakovic, N. Radic, B. Grbic, V. Dondur, M. Mitric, D. Randjelovic, D. Stoychev, P. Stefanov, *Appl. Surf. Sci.* **255** (2008) 3049
4. A. L. Ahmad, N. N. N. Mustafa, *J. Hydrogen Energ.* **32** (2007) 2010
5. H. Klym, A. Ingram, I. Hadzaman, O. Shpotyuk, *Ceram. Int.* **40** (2014) 8561
6. J. Čejka, *Appl. Catal., A* **254** (2003) 327
7. H. Arai, M. Machida, *Appl. Catal., A* **138** (1996) 161
8. A. C. Pierre, *Ceram. Int.* **23** (1996) 229
9. N. Radić, B. Grbić, Lj. Rožić, T. Novaković, S. Petrović, D. Stoychev, P. Stefanov, *J. Non-Cryst. Solids* **357** (2011) 3592
10. M. Ozawa, Y. Nishio, *J. Alloy. Compd.* **374** (2004) 397
11. Y. Wang, J. Wang, M. Shen, W. Wang, *J. Alloy. Compd.* **467** (2009) 405
12. P. Burtin, J. P. Brunelle, M. Pijolat, M. Soustelle, *Appl. Catal.* **34** (1987) 225
13. P. Exter, L. Winnubst, T. H. P. Leuwernik, A. J. Burgg, *J. Am. Ceram. Soc.* **77** (1994) 2376
14. M. Riad, *Appl. Catal., A* **327** (2007) 13
15. M. Crişan, M. Zaharescu, V. D. Kumari, M. Subrahmanyam, D. Crişan, N. Drăgan, M. Răileanu, M. Jitianu, A. Rusu, G. Sadanandam, J. K. Reddy, *Appl. Surf. Sci.* **258** (2011) 448
16. A. Khaleel, S. Al-Mansouri, *Colloids Surfaces, A* **369** (2010) 272
17. G. S. Walker, D. R. Pyke, C. R. Werrett, E. Williams, A. K. Bhattacharya, *Appl. Surf. Sci.* **147** (1999) 228
18. W. L. Huang, S. H. Cui, K. M. Liang, Z. F. Yuan, S. R. Gu, *J. Phys. Chem. Solids* **63** (2002) 645
19. S. Da Ros, E. Barbosa-Coutinho, M. Schwaab, V. Calsavara, N. R. C. Fernandes-Machad, *Mater. Charact.* **80** (2013) 50
20. B. Huang, C. H. Bartholomew, B. F. Woodfield, *Micropor. Mesopor. Mat.* **177** (2013) 37
21. S. Ghanizdeh, X. Bao, B. Vaidhyanathan, J. Binner, *Ceram. Int.* **40** (2014) 1311
22. A. S. Kaigorodov, V. R. Khrustov, V. V. Ivanov, A. I. Medvedev, A. K. Shtol'ts, *Sci. Sinter.* **37** (2005) 35
23. A. Vatanara, A. R. Najafabadi, K. Gilani, R. Asgharian, M. Darabi, M. Rafiee-Tehrani, *J. Supercrit. Fluid.* **40** (2007) 111
24. S. Menecier, J. Jarrige, J. C. Labbe, P. Lefort, *J. Eur. Ceram. Soc.* **27** (2007) 851
25. P. Wang, Z. Wang, Z. Wu, *Chem. Eng. J.* **193**–**194** (2012) 50
26. A. S. Guzun, M. Stroescu, S. I. Jinga, G. Voicu, A. M. Grumezescu, A. M. Holban, *Mat. Sci. Eng., C* **42** (2014) 280
27. B. E. Yoldas, *Am. Ceram. Soc. Bull.* **54** (1975) 289

28. F. Rouquerol, J. Rouquerol, K. S. W. Sing, P. Llewellyn, G. Maurin, *Adsorption by Powders and Porous Solids, Principles, Methodology and Applications*, Academic Press, New York, 2012
29. B. C. Lippens, B. G. Linsen, J. H. de Boer, *J. Catal*. **3** (1964) 32
30. K. Sing, D. Everet, R. Haul, L. Moscou, R. Pierotti, J. Rouquerol, T. Siemieniewska, *Pure Appl. Chem*. **57** (1985) 603
31. P. Orosco, L. Barbosa, M. C. Ruiz, *Mater. Res. Bull*. **59** (2014) 337.